JOURNAL OF APPLIED PHYSICS **104**, 024315 (2008)

Nanoscale capacitance microscopy of thin dielectric films

G. Gomila,[a] J. Toset, and L. Fumagalli
Caracterització Bioelèctrica a la Nanoescala, Institut de Bioenginyeria de Catalunya (IBEC),
CIBER-Bioingeniería, Biomateriales y Nanomedicina, and Departament d'Electrònica,
Universitat de Barcelona, Martí i Franquès, 1, 08028-Barcelona, Spain

(Received 26 February 2008; accepted 16 May 2008; published online 25 July 2008)

We present an analytical model to interpret nanoscale capacitance microscopy measurements on thin dielectric films. The model displays a logarithmic dependence on the tip-sample distance and on the film thickness-dielectric constant ratio and shows an excellent agreement with finite-element numerical simulations and experimental results on a broad range of values. Based on these results, we discuss the capabilities of nanoscale capacitance microscopy for the quantitative extraction of the dielectric constant and the thickness of thin dielectric films at the nanoscale. © *2008 American Institute of Physics*. [DOI: 10.1063/1.2957069]

I. INTRODUCTION

Nanoscale capacitance microscopy[1–4] (NCM) is an emerging technique that measures the capacitance between an atomic force microscope (AFM) tip and the metallic, semiconductor, or dielectric material deposited on a conductive substrate [Fig. 1(a)]. For thin dielectric films, the power of NCM resides in the ability to quantify intrinsic properties, including film thickness[5] and dielectric constant,[6] with lateral spatial resolution well beyond the limit of conventional ellipsometry, reflectance spectroscopy,[7] and capacitance metrology.[8,9]

In two recent papers,[6,10] we have demonstrated the quantitative measurement of the dielectric constant and the thickness of thin insulating films at the nanoscale. To extract these parameters, we have used the following logarithmic expression of the capacitance probed by the nanometric tip apex on the thin dielectric film,

$$C_{\text{apex}}^{\text{dielectric}}(z,\varepsilon_r,h) = 2\pi\varepsilon_0 R \ln\left[1 + \frac{R\cdot(1-\sin\theta_0)}{z + h/\varepsilon_r}\right], \qquad (1)$$

where ε_0 is the vacuum dielectric constant, ε_r the relative dielectric constant of the film, h the thickness of the film, z the apex-film separation distance, R the effective apex radius, and θ_0 the cone angle of the tip [see Fig. 1(b)]. However, a theoretical assessment of the origin and range of applicability of Eq. (1) has not been provided yet.

In the present paper, we precisely address this issue by presenting a theoretical discussion on the origin and the range of applicability of Eq. (1). We demonstrate that this analytical model is in excellent agreement with finite-element numerical simulations in a wide range of parameters and sizes of the system. Based on these results, we will discuss the capabilities and range of applicability of NCM for the quantitative characterization of thin dielectric films at the nanoscale.

We note that an analytical model for the tip-sample capacitance on a dielectric film, besides a direct use in NCM, is of great importance also in the context of electrostatic force microscopy and scanning capacitance microscopy (SCM),[11] in which previous studies[12–14] have mostly restrict themselves to numerical simulations and not fully addressed the analytical modeling.

II. APEX CAPACITANCE MODEL FOR A THIN DIELECTRIC FILM

A. Theoretical derivation

In NCM, the measured capacitance is the sum of two contributions shown in Fig. 1(a), namely, the apex capacitance C_{apex} sensed by the very end of the probe and the stray capacitance C_{stray} associated with the tip cone, the cantilever, and the whole AFM probe assembly. Only the apex contribution depends on the local properties of the sample,[2,6,10] as will be clearly shown later, and, hence, it is the single contribution that needs to be analytically modeled in a precise way. The remaining contributions conform the stray capacitance contribution that can be subtracted from the experiments following an appropriate calibration procedure as previously reported.[1,6,10]

In order to arrive at an analytical expression for the apex capacitance in the presence of a thin dielectric film, we will restrict ourselves to the model system depicted in Fig. 1(b). The sharp metallic tip is modeled as a truncated cone of height H and aperture angle θ_0 ended with a spherical sur-

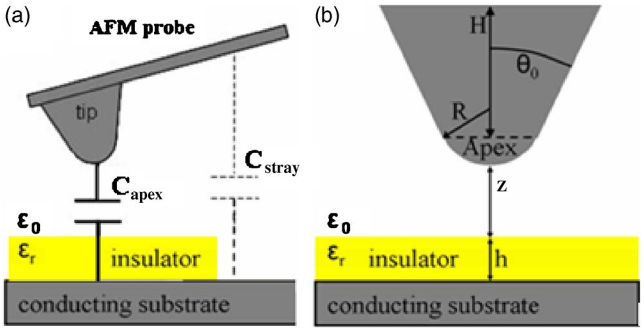

FIG. 1. (Color online) Schematic representation of (a) a nanoscale capacitance measurement and (b) the tip-sample system as modeled in our numerical calculations.

---

[a] Electronic mail: ggomila@el.ub.es.

0021-8979/2008/104(2)/024315/8/$23.00

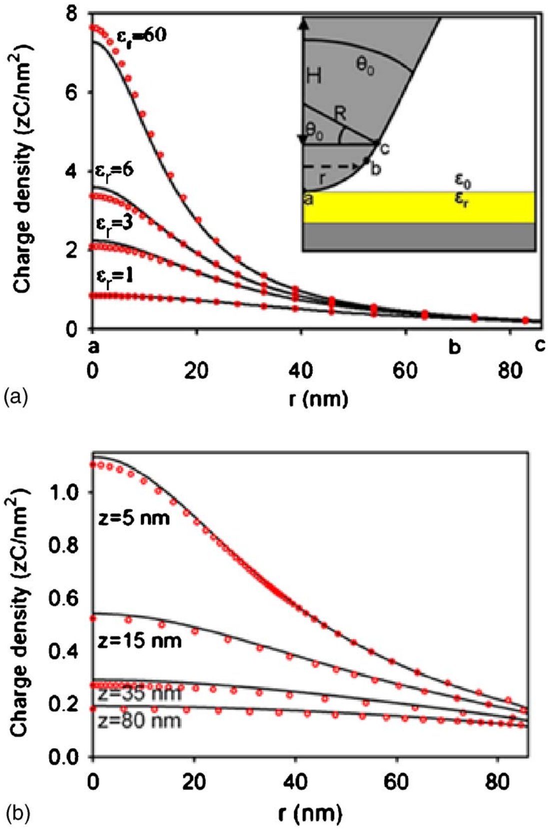

FIG. 2. (Color online) Surface charge density distribution obtained from numerical simulation (symbols) and the analytical model (continuous line) on the tip surface as a function of the radial distance r from the axis (film thickness $h=10$ nm, tip radius $R=100$ nm, cone angle $\theta_0=30°$, and height $H=16$ μm, voltage difference V=1 V). (a) Calculation for the tip in contact with the dielectric film ($z\sim 0$ nm) and different relative dielectric constants. Inset: schematic representation of the model system showing relevant positions (a, b, and c) on the apex; (b) calculation for the tip at different distances from a dielectric film of relative dielectric constant $\varepsilon_r=3$.

face of radius R. The apex capacitance is mathematically defined here as the capacitance associated with the spherical area of the apex. The tip is located at a distance z from a thin dielectric layer in air atmosphere of vacuum dielectric constant ε_0. The film, deposited on a conductive substrate, has thickness h and relative dielectric constant ε_r. We will considered here only thin films, with $h \ll H$, which allows us to disregard the effect of the cantilever on the electric field distribution, as demonstrated by Sacha *et al.*[15] For simplicity, we assume the dielectric film (or any nanostructure on it) to be homogeneous and with a lateral extension larger than the apex radius. If these conditions are not satisfied, issues related to the lateral spatial resolution of the capacitance measurement may appear, which will not be discussed here.

When a voltage difference is applied between the tip and the bottom electrode, the electric charge distributes itself over the tip surface as to make it an equipotential surface. The charge distribution is not uniform due to the close proximity of the dielectric film. Its spatial distribution depends not only on geometrical parameters of the system, R, θ_0, and the tip-film distance z but also on the intrinsic properties of the dielectric film, h and ε_r.

In Fig. 2 we plot the charge density distribution (symbols) on the tip surface as a function of the radial distance r from the axis, numerically calculated for different relative dielectric constants [Fig. 2(a)] and tip-film distances [Fig. 2(b)], in the case of a dielectric film of thickness $h=10$ nm and for 1 V applied. The tip parameters are those of a typical conductive probe for scanning force microscopy with radius of $R=100$ nm, cone angle $\theta_0=30°$, and height $H=16$ μm (the default parameters of the system if not otherwise specified). The curves have been obtained by using the electrostatic module in the finite-element software COMSOL MULTIPHYSICS. We note in Fig. 2 that only the charge density in the apex region is sensitive to the relative dielectric constant value [Fig. 2(a)] and to the tip-sample distance [Fig. 2(b)], while the charge density corresponding to the remaining part of the probe is almost insensitive to these parameters. This fact justifies the assumption that only the apex of the tip is sensitive to the local properties of the thin film, thus justifying the inclusion of the cone contribution into the stray capacitance term.

Remarkably the charge distribution on the probe surface obtained numerically can be quantitatively described by the following simple analytical model:

$$\sigma_{\text{apex}}(r;z,R,\theta_0,h,\varepsilon_r) = \frac{\alpha(\theta_0)\varepsilon_0}{R} + \frac{\varepsilon_0}{z + h/\varepsilon_r + R - \sqrt{R^2 - r^2}}, \tag{2}$$

where σ_{apex} is the surface charge density (per volt applied) and α is a constant term *dependent only on the cone angle*, with the remaining parameters already defined. By fitting the numerical simulations with α as single fitting parameter, we obtain $\alpha(30°)=0.23$ and, for different cone angles, $\alpha(10°)=0.45$ and $\alpha(45°)=0.16$. The agreement between Eq. (2) and the numerical simulations is excellent in the whole range of distances and parameters, as shown in Fig. 2. A small discrepancy is observed only at the very end of the tip. As will be seen later, this is not significant in terms of the apex capacitance, which can be obtained by integrating the charge density over the whole apex surface.

Equation (2) is interpreted as follows: the first term is reminiscent from the uniform charge distribution of an isolated probe, as suggested in Ref. 12, while the second term corresponds to the charge density on an infinite parallel-plate capacitor of plate separation $z+h+R-\sqrt{R^2-r^2}$ partially filled with a dielectric material of thickness h and relative dielectric constant ε_r. However, this simple interpretation should be taken with caution. On the one hand, the first term does not correspond quantitatively to the value of the isolated probe, as we have verified for the case of a conducting sphere (not shown here). On the other hand, in the infinite parallel-plate approximation the magnitude of the electric field is uniform in the perpendicular direction to the plates, whereas the computed electric fields here show a remarkable dependence on the vertical spatial variable. In any case, this simple interpretation allows one arriving at Eq. (2) in a rather direct way.

The apex capacitance is calculated from the surface charge density distribution (per volt applied) as

$$
\begin{aligned}
C_{\text{apex}} &= \int_{S_{\text{apex}}} \sigma_{\text{apex}} dS \\
&= \int_0^{R\cos\theta_0} \left[\frac{\alpha(\theta_0)\varepsilon_0}{R} + \frac{\varepsilon_0}{z + R + h/\varepsilon_r - \sqrt{R^2 - r^2}} \right] \\
&\quad \times \frac{2\pi R r}{\sqrt{R^2 - r^2}} dr, \qquad (3)
\end{aligned}
$$

which gives

$$
C_{\text{apex}} = 2\pi\varepsilon_0 R \ln\left\{ 1 + \frac{R[1 - \sin(\theta_0)]}{z + \dfrac{h}{\varepsilon_r}} \right\} + C_0(R,\theta_0), \qquad (4)
$$

with

$$
C_0(R,\theta_0) = 2\pi\varepsilon_0 R \alpha(\theta_0)(1 - \sin\theta_0), \qquad (5)
$$

where all parameters appearing in Eqs. (3)–(5) have been previously defined. Equation (4) coincides with Eq. (1) given in the Introduction except for an additive constant term. As we will see later on, this term is necessary to fit the finite-element simulations, but it is irrelevant from an experimental point of view, where only variations (and not the absolute values) of the apex capacitance with respect to the stray capacitance can be measured.

Equation (4) provides the dependency of the apex capacitance as a function of the apex geometry (here represented by R and θ_0), the intrinsic properties of the dielectric film (h and ε_r), and the tip-film separation z. Equation (4) displays a remarkably simple dependence of the apex capacitance on the film parameters through the ratio h/ε_r. It is also worth noting the logarithmic dependence of Eq. (4) on the dielectric ratio h/ε_r and tip-sample distance z, which essentially departs from the parallel-plane capacitor behavior that would show stronger sensitivity to the local dielectric properties. In the limit of a metallic sample, obtained either when $h=0$ or $\varepsilon_r \to \infty$, Eq. (4) reduces to

$$
C_{\text{apex}}^{\text{metal}} = 2\pi\varepsilon_0 R \ln\left\{ 1 + \frac{R[1 - \sin(\theta_0)]}{z} \right\} + C_0(R,\theta_0), \qquad (6)
$$

which is the expression proposed by Hudlet *et al.*[16] for a metallic sample except for the (experimentally irrelevant) constant term (see Ref. 17 for an experimental validation of Hudlet *et al.* formula).

B. Numerical validation

To analyze the range of validity of the analytical expression proposed for the apex capacitance, we have compared the behavior of Eq. (4) to finite-element numerical simulations for different parameters and sizes of the tip-dielectric film system. The goodness of Eq. (4) is studied varying the geometrical size of the probe (R and θ_0), the intrinsic properties of the thin film (h and ε_r), and the tip-film distance z. In the following, we will assume $h=10$ nm, $R=100$ nm, $\theta_0=30°$, and $\varepsilon_r=3$, if not otherwise specified.

Figure 3 shows the apex capacitance as a function of the apex-dielectric film separation z for different radii, $R=30$, 100, and 200 nm, and relative dielectric constants $\varepsilon_r=1$, 3, and 6. The numerically computed capacitance and its dependence on the relative dielectric constant and apex radii are qualitatively similar to the one described in a previous numerical analysis.[12] The theoretical values given by Eq. (4) provide a remarkably excellent agreement with the numerical simulations in all cases by using $\alpha(30°)=0.23$. Similar agreement is obtained when varying the film thickness, e.g., $h=30$ nm and $h=100$ nm (not shown here).

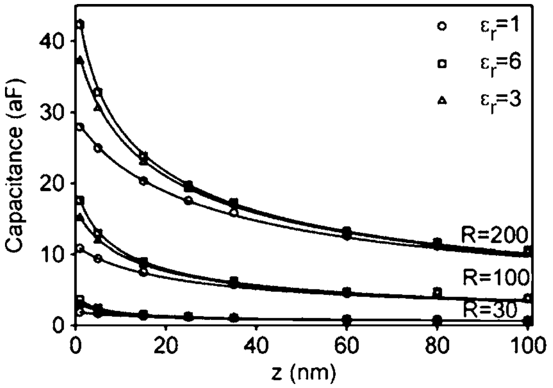

FIG. 3. Capacitance-distance curves on a film of thickness $h=10$ nm calculated for different radii ($R=30$, 100, and 200 nm) and film relative dielectric constants ($\varepsilon_r=1$, 3, and 6). Symbols: numerical simulations. Solid lines: theoretical curves given by Eq. (4) with $\alpha(30°)=0.23$.

The cone angle dependence is also adequately reproduced by the analytical model. Figure 4 shows the apex capacitance as a function of the apex-dielectric film separation z for three different cone angles $\theta_0=10°$, 30°, and 45°. Again the agreement between numerical and analytical calculations is excellent, provided the corresponding values of α reported in Sec. II A are used.

Finally, Fig. 5 gives the apex capacitance as a function of the film thickness and of the relative dielectric constant, when the tip apex is in close proximity to the dielectric film ($z=0.1$ nm, not strictly $z=0$ nm to avoid some simulation difficulties). Again the theoretical results and the numerical simulations are in excellent agreement in the whole range of parameters here considered. Even in the limits of high rela-

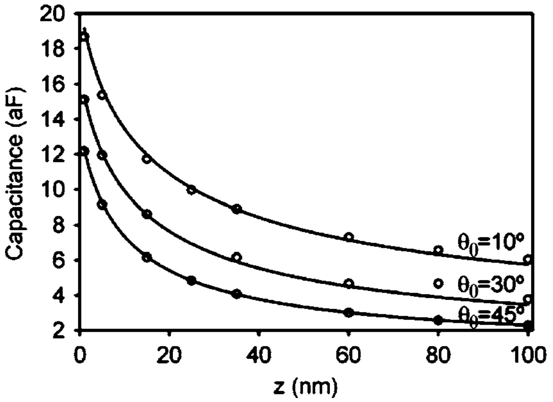

FIG. 4. Capacitance-distance curves calculated on a film of thickness $h=10$ nm and relative dielectric constant $\varepsilon_r=3$ for a probe of radius $R=100$ nm calculated for different cone angles 10°, 30°, and 45°. Symbols: numerical simulations. Solid lines: theoretical curves given by Eq. (4) with $\alpha(10°)=0.45$, $\alpha(30°)=0.23$, and $\alpha(45°)=0.16$.

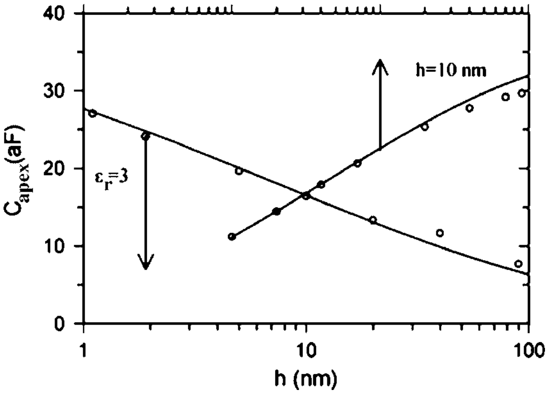

FIG. 5. Apex capacitance calculated for the probe in close contact with a dielectric film as a function of the relative dielectric constant ε_r for a fixed dielectric thickness of $h=10$ nm (upper horizontal axis) and as a function of dielectric thickness for a fixed relative dielectric constant of $\varepsilon_r=3$ (bottom horizontal axis) (tip radius $R=100$ nm and cone angle 30°). Symbols: numerical simulations. Solid lines: theoretical curves given by Eq. (4) with $\alpha(30°)=0.23$.

tive dielectric constant (up to $\varepsilon_r=100$) or thick dielectric films (up to $h=100$ nm), only slight deviations are obtained (below 1–2 aF).

These numerical simulations fully validate the analytical model derived in Sec. II A and demonstrate that the model is extremely accurate in a broad range of parameter values, including apex-film distance z from contact to 100 nm, film thickness h from 1 nm up to 100 nm, relative dielectric constant ε_r from 1 to 100, apex radius R from 30 to 200 nm, and cone angles θ_0 from 10° to 45°.

III. EXTRACTION OF NANOSCALE DIELECTRIC FILM PROPERTIES

Once demonstrated the broad validity of the simple analytical model of Eq. (4), we can now discuss on a theoretical basis the capabilities and limitations of NCM for quantitative characterization of thin dielectric films under realistic experimental conditions. Equation (4) can be used to extract the dielectric ratio h/ε_r and, from this, the film thickness h or relative dielectric constant ε_r at the nanoscale, depending on the measurement approach. Among the various strategies that can be used, we will discuss in what follows two representative experimental methods: (a) capacitance-distance curve measurements $C(Z)$ and (b) capacitance profile measurements $C(X)$, where Z and X are the vertical and the fast scan direction, respectively.

A. Capacitance versus distance measurements

In Ref. 6 we have demonstrated that by performing calibrated $C(Z)$ curves on a homogeneous and uniformly thick dielectric film (see Fig. 6 below), the ratio h/ε_r can be extracted in a very quantitative way at the nanoscale. From Eq. (4), we can model the apex capacitance variation measured while approaching the tip to the film as

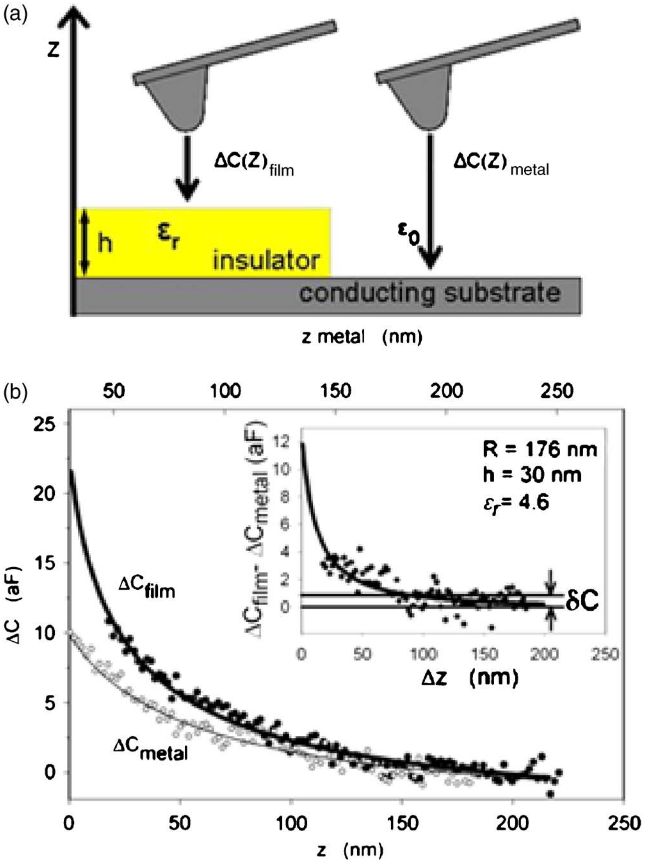

FIG. 6. (Color online) (a) Schematic representation of a nanoscale capacitance-distance experiment on a thin dielectric film. (b) Experimental apex capacitance (black circles) and fitting to Eq. (7) (thick line) as function of tip-sample distance on a SiO_2 thin film of thickness $h=30$ nm. The calibration curve (white circles) performed on a metal region not covered by the film is also reported and fitted to Eq. (8) (thin line). The horizontal axis for this curve has been shifted an amount equal to the dielectric film thickness to compare the curves at equal interelectrode distance. Extracted parameters: $R=176$ nm and $\varepsilon_r=4.6$ (with $\theta_0=30°$) Inset: measured (circles) and fitting (line) difference between the $C(Z)$ curve on the film and the one on the metal at equal interelectrode distances (all measurements have been performed with an applied ac voltage of 1 V amplitude and 60 kHz frequency).

$$\Delta C_{\text{apex}}^{\text{dielectric}} = 2\pi\varepsilon_0 R \ln\left\{\frac{1+\dfrac{R[1-\sin(\theta)]}{z+h/\varepsilon_r}}{1+\dfrac{R[1-\sin(\theta)]}{z_0+h/\varepsilon_r}}\right\}, \tag{7}$$

where z_0 is the initial apex-film distance. While z_0 can be precisely assessed through a simultaneous acquired force-distance curve, the geometrical parameters of the tip, R and θ_0, can be accurately calibrated by taking a similar $C(Z)$ curve on a metal surface and fitting it to the capacitance variation expression for a metallic substrate obtained from Eq. (6), namely,

$$\Delta C_{\text{apex}}^{\text{metalic}} = 2\pi\varepsilon_0 R \ln\left\{\frac{1+\dfrac{R[1-\sin(\theta)]}{z}}{1+\dfrac{R[1-\sin(\theta)]}{z_0}}\right\} \tag{8}$$

(see Ref. 6 for details). Therefore, the only unknown parameter in Eq. (7) is the dielectric ratio h/ε_r, which can be extracted by fitting the experimental data. From the dielectric ratio, either h or ε_r can be obtained, provided one of the two parameters has a known value.

An example of such a procedure is illustrated in Fig. 6(b) where an experimental capacitance distance curve taken on a $\mathrm{SiO_2}$ thin film of $h=30$ nm is shown. For comparison and tip calibration purposes, an approach curve measured on a metal region not covered by the film is also shown. The horizontal axis for this last curve has been shifted an amount equal to the film thickness h to compare the two $C(Z)$ curves at equal interelectrode distance. As can be seen the two experimental curves are in excellent agreement with the analytical models in Eqs. (7) and (8), respectively, giving a tip radius $R \sim 176 \pm 14$ and a relative dielectric constant $\varepsilon_r \sim 4.6 \pm 1.2$ (the cone angle is kept to 30°). The precision of the extracted parameters is set essentially by the capacitance noise of the instrument δC (here, $\delta C \sim 0.7$ aF) and the size of the apex radius.

The $C(Z)$ approach for the extraction of the intrinsic properties of the thin films as outlined above can be applied as long as (i) the difference between the curve measured on the dielectric film and the one on the bare metal at equal interelectrode distances is larger than the capacitance noise δC [inset of Fig. 6(b)] and (ii) the range of distances in which the instrument detects the dielectric film is sufficiently large for a meaningful fitting. This distance interval of sensitivity can be defined as $\Delta z = z_{\delta C} - z_{jc}$, where the lower limit z_{jc} is the jump-to-contact distance and the higher, $z_{\delta C}$, is the maximum distance at which the instrument is able to distinguish the dielectric film from the metallic substrate. The maximum distance of sensitivity $z_{\delta C}$ can be determined by equalizing the capacitance noise to the difference between the curve on the dielectric film and the one on the metal at equal interelectrode distance as

$$\delta C = \Delta C_{\text{apex}}^{\text{dielectric}}(z_{\delta C}) - \Delta C_{\text{apex}}^{\text{metal}}(z_{\delta C}). \tag{9}$$

According to this definition, the maximum sensitivity distance in the experiments reported in Fig. 6 is roughly 75 nm (see the inset). On a theoretical basis, Eq. (9) reads

$$\delta C = 2\pi\varepsilon_0 R \ln\left[\frac{1+\dfrac{R[1-\sin(\theta)]}{z_{\delta C}+h/\varepsilon_r}}{1+\dfrac{R[1-\sin(\theta_0)]}{z_{\delta C}+h}}\right] - 2\pi\varepsilon_0 R \ln\left[\frac{1+\dfrac{R[1-\sin(\theta_0)]}{z_0+h/\varepsilon_r}}{1+\dfrac{R[1-\sin(\theta_0)]}{z_0+h}}\right], \tag{10}$$

where the second term of Eq. (10) is negligible, provided that $z_0 \gg h$.

By imposing a given value to $z_{\delta C}$, Eq. (10) can be used conversely to define the region of the R versus h plane, in which the setup is expected to be sensitive to the dielectric layer of relative dielectric constant ε_r below the tip at a distance $z_{\delta C}$. From this type of plot one can evaluate whether the experiment is meaningful under given experimental conditions.

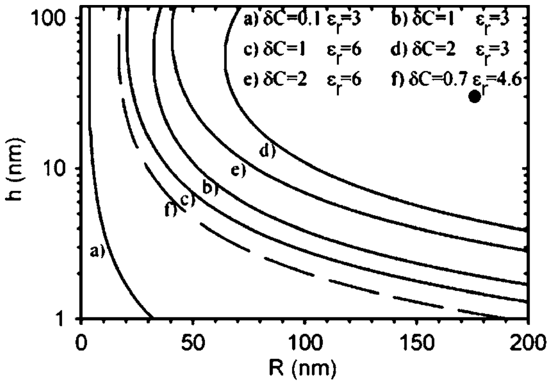

FIG. 7. Theoretical sensitivity plot in the thickness h vs radius R plane, showing the conditions required to detect a thin dielectric film in a capacitance-distance experiment. For each curve, the sensitive region is to the right. Calculations are obtained from Eq. (10) for different relative dielectric constants ($\varepsilon_r=3,6$) and capacitance noise ($\delta C=0.1,1,2$ aF), and fixed parameters $\theta_0=30°$, $z_{\delta c}=10$ nm, and $z_0=100$ nm. The dashed line and the free dot correspond to the experimental situation shown in Fig. 6(b).

Figure 7 shows a representative plot for the case of $\theta_0=30°$, $z_{\delta C}=10$ nm, capacitance noise $\delta C=0.1$, 1, and 2 aF, relative dielectric constant $\varepsilon_r=3$ and 6, and for an initial distance equal to $z_0=100$ nm. We can see that in each case, for a given capacitance noise of the instrument, there exits a minimum radius $R_{\min}$ below which the experiment is not sensitive to the dielectric film irrespectively of the thickness and relative dielectric constant. The value of $R_{\min}$ strongly depends on the capacitance noise level and relative dielectric constant to be detected. For instance, for an instrument with capacitance noise of $\delta C=2$ aF and a dielectric film of $\varepsilon_r=3$, one would need a tip radius of $R > R_{\min}=65$ nm to be sensitive at 10 nm tip-film distance. Instead, for 1 aF noise level, one would need $R_{\min}=33$ nm, and for 0.1 aF, only $R_{\min}=3$ nm. In addition, for a given radius, there exists a range of film thicknesses that are detectable, which also depends on capacitance noise and relative dielectric constant. As an example, for $R=70$ nm, $\delta C=2$ aF, and $\varepsilon_r=3$, the measurable range of thickness is between $h_{\min}=30$ nm and $h_{\max}=111$ nm.

In view of these results, the experimental noise level of NCM is fundamental. Existing instruments can attain capacitance resolution down to 1 aF in a reasonable timescale. Therefore, they are able to detect ultrathin dielectric films by capacitance-distance curves in most cases, but with a trade-off between spatial resolution (apex radius), relative dielectric constant, and film thickness. Molecular film thicknesses ($h < 2$ nm) currently lie at the frontier of the state of the art, requiring very large tip radius. To access molecular films with acceptable lateral resolution (40–50 nm), improvement of instrumental capacitance resolution below 0.1 aF is necessary. The tip-capacitance formula can also be used to test how precise is the measured relative dielectric constant using the capacitance-distance approach. To determine whether the measurement is able to distinguish to close values of the dielectric constant, say ε_1 from ε_2, one can modify Eq. (10) as

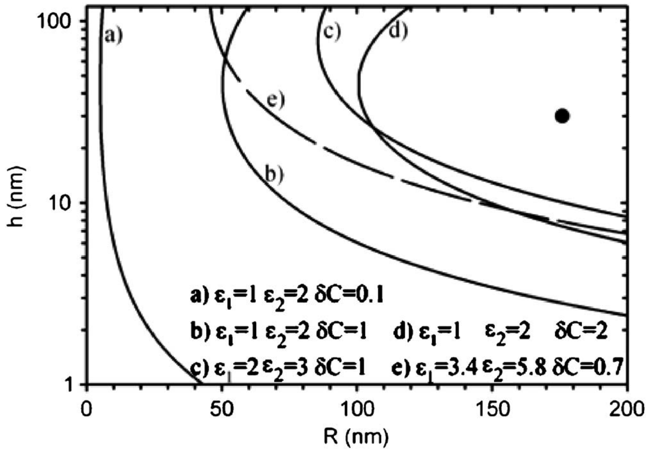

FIG. 8. Theoretical sensitivity plot in the thickness h vs radius R plane showing the conditions required to set the value of the dielectric film in a given interval (ε_1 and ε_2) by a capacitance-distance experiment. For each curve, the sensitive region is to the right. Calculations are obtained from Eq. (11) with different capacitance noises ($\delta C=0.1, 1, 2$ aF) and fixed parameters $\theta_0=30°$, $z_{\delta c}=10$ nm, and $z_0=100$ nm. The dashed line and the free dot correspond to the experimental situation shown in Fig. 6(b).

$$\delta C = 2\pi\varepsilon_0 R \ln\left[\frac{1+\dfrac{R[1-\sin(\theta)]}{z_{\delta C}+h/\varepsilon_2}}{1+\dfrac{R[1-\sin(\theta)]}{z_{\delta C}+h/\varepsilon_1}}\right] - 2\pi\varepsilon_0 R \ln\left[\frac{1+\dfrac{R[1-\sin(\theta_0)]}{z_0+h/\varepsilon_2}}{1+\dfrac{R[1-\sin(\theta_0)]}{z_0+h/\varepsilon_1}}\right]. \tag{11}$$

Figure 8 gives the sensitivity plot in the R-h plane for three couples of relative dielectric constants (1 and 2, 2 and 3, and 3 and 4) for various capacitance noises. As can be seen in Fig. 8, the sensitivity regions considerably reduce when trying to determine the relative dielectric constant in a given interval of values. They move toward thicker films and larger radius for increasing values of the relative dielectric constant. Therefore, existing instrumentation can set the relative dielectric constant value with a reasonable precision for low relative dielectric constants (say $\varepsilon_r<5$), but as before with a trade-off between precision, tip radius, and sample thickness. Nanoscale capacitance-distance experiment reported in Fig. 7(b) satisfies the requirements to be sensitive to the presence and able to set the value of the dielectric constant in a prefixed range of values, as illustrated in Figs. 8 and 9 by the location of the big dot.

B. Capacitance profile measurement

In Ref. 10 we demonstrated that simultaneous capacitance and topographic profiling measurements on a micro/nanopatterned dielectric film allow one estimating in a very quantitatively way the thickness of the film at the nanoscale with high vertical resolution.

In a capacitance profile experiment, the topography and local capacitance variations are measured simultaneously with the tip in contact with the film, as sketched in Fig. 9(a).

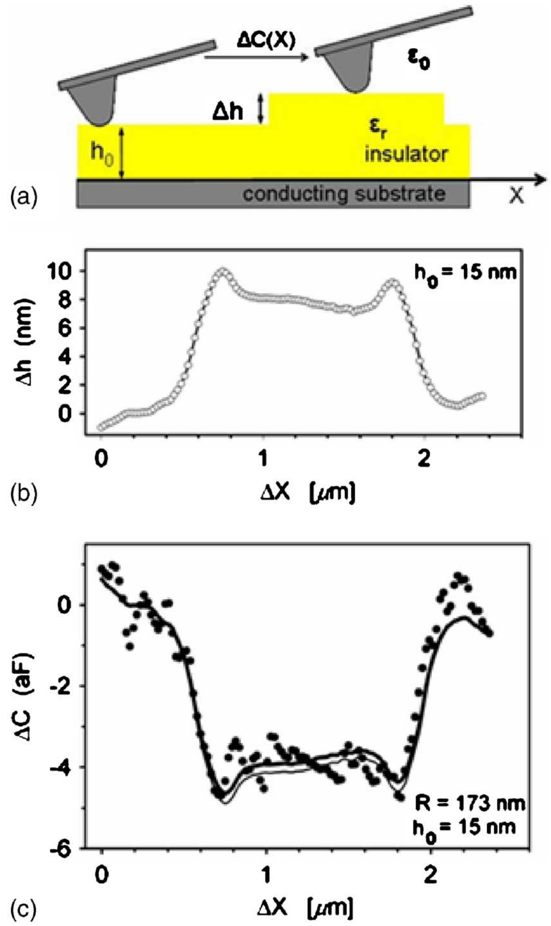

FIG. 9. (Color online) (a) Schematic representation of a nanoscale capacitance profiling measurement on a homogeneous dielectric film with topographic variations (step of height Δh). (b) Experimental topography and (c) local capacitance profile measured on a nanostructured SiO_2 thin film of unknown base thickness h_0 (symbols). The thick solid line corresponds to the prediction of Eq. (12) with a base thickness $h_0\sim 15$ nm (and $\varepsilon_r=4$) calculated with the experimentally calibrated radius $R\sim 173$ nm. The thin solid line corresponds to the approximate expression for the capacitance variation in Eq. (13), which is independent of the relative dielectric constant value (measurements done with applied an ac voltage of 1 V amplitude and 93 kHz frequency).

In the simple case of a *homogeneous* film of relative dielectric constant ε_r with some thickness variations (a step or simply the sample roughness), the measured variation in the apex capacitance with respect to a reference location on the film, x_0, can be modeled as

$$\Delta C_{\text{apex}}^{\text{dielectric}} = 2\pi\varepsilon_0 R \ln\left\{\frac{1+\dfrac{R(1-\sin\theta_0)}{[h(x_0)+\Delta h(x)]/\varepsilon_r}}{1+\dfrac{R(1-\sin\theta_0)}{h(x_0)/\varepsilon_r}}\right\}, \tag{12}$$

where $h(x)=h(x_0)+\Delta h(x)$ and $h(x_0)$ are the film thickness at locations x and x_0, respectively. Equation (12) is deduced from Eq. (7) by setting the tip-film distance at zero, $z=0$ nm. Note that topography alone can give information on thickness variations, i.e., $\Delta h(x)$, but, in general, it does not give information on the total sample thickness, that is, it does not inform on the base thickness of the sample $h(x_0)$. A combination of topography and nanoscale profiling allows one

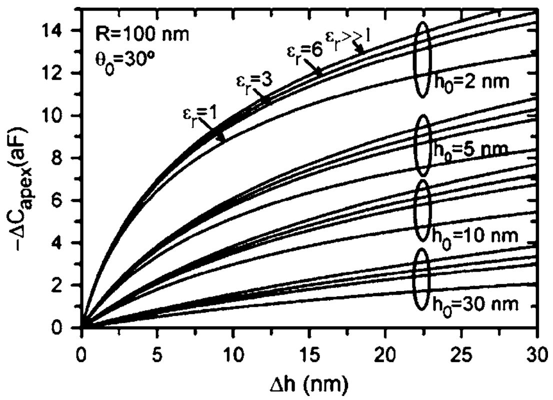

FIG. 10. Theoretical estimation of the change in apex capacitance when taking a profile on a dielectric step as a function of the step height Δh for various bare thicknesses h_0 and relative dielectric constants ε_r (fixed parameters $\theta_0=30°$ and $R=100$ nm).

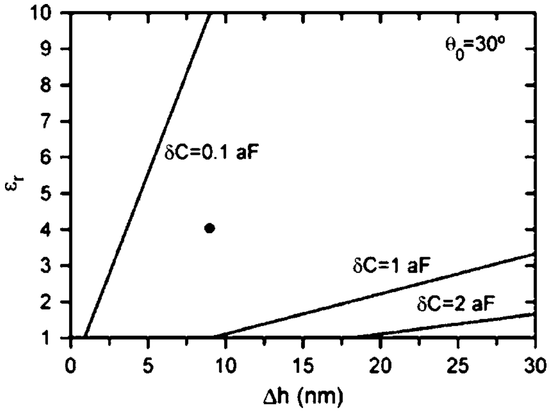

FIG. 11. Theoretical sensitivity plot in the step height Δh vs relative dielectric constant ε_r plane, showing the regions under which capacitance profiles are sensitive to the value of the relative dielectric constant (to the right of the lines in each case). The cone angle is kept to 30° and different capacitance noise levels are considered ($\delta C=0.1, 1, 2$ aF). Results are independent of the radius R and film thickness h. The free dot corresponds to the experimental conditions in Fig. 9 with $\delta C=1$ aF.

obtaining this value (provided the relative dielectric constant is known, see below about this point). To this end one measures the film topography simultaneously to the capacitance variation, and then makes use of Eq. (12) with a calibrated tip radius (and known relative dielectric constant).

An example of this procedure is illustrated in Fig. 9, where simultaneous capacitance [Fig. 9(c)] and topography [Fig. 9(b)] profiles were simultaneously measured on a nanostructured SiO_2 thin film, displaying a steplike variation in its thickness. The measured capacitance variation shown in Fig. 9(c) is the local contribution, accurately extracted after calibration of the vertical and lateral stray contributions, as detailed in Refs. 1, 2, and 6. The tip radius R was precisely calibrated ($R\sim 173$ nm) by fitting to Eq. (8) $C(Z)$ curves taken on a metal region not covered by the film, as described before. The capacitance profile was fitted to Eq. (12) with a single unknown parameter (the base thickness h_0) giving $h_0 \sim 15$ nm in complete agreement with an independent topographic measurement performed at the edge of the structure taking as reference the metal substrate. The relative dielectric constant was taken to be $\varepsilon_r=4$ although, as we will see below, in this case the result was almost independent of this precise value. These results show how by means of simultaneous topographic and capacitance profiles we can extract the film thickness at the nanoscale in a very quantitative way.

It is worth analyzing the sensitivity of the extraction procedure sketched above. To this end, we plot in Fig. 10 the theoretical apex capacitance variation predicted by Eq. (12) as a function of the step height Δh for various base thicknesses h_0 and relative dielectric constants ε_r of the film. The apex radius and the cone angle are kept fixed to $R=100$ nm and $\theta_0=30°$, respectively.

We see that the sensitivity of the apex capacitance to the thickness h_0 and step height Δh is remarkable, while it is comparatively lower to the value of the relative dielectric constant. Indeed, for a given h_0 and Δh, the increase of capacitance with ε_r is rather small 1–2 aF at most in the present case. This means that the capacitance profile measurement on thin homogeneous films is a very good method for thickness measurement in a wide range of values (roughly h, $\Delta h < 30$ nm for $R=100$ nm), but not for relative dielectric constant extraction. We can precise this statement mathematically by noting that for $\varepsilon_r R[1-\sin(\theta_0)] \gg h+\Delta h, h_0$, Eq. (12) can be approximated to

$$\Delta C_{\rm apex}^{\rm dielectric} \approx 2\pi\varepsilon_0 R \ln\left(\frac{h_0}{h_0+\Delta h}\right) + O(1), \qquad (13)$$

which is dependent only on the thicknesses and the apex radius, but not on the relative dielectric constant, whose contribution will only appear as a first-order correction term. The thin line in Fig. 9(c) and the lines for $\varepsilon_r \gg 1$ in Fig. 10 correspond to the approximate expression in Eq. (13), thus illustrating the goodness of the approximation. To be sensitive to the relative dielectric constant value in a capacitance profiling experiment, one would need a capacitance noise level δC lower than the first order correction term to Eq. (13), that is,

$$2\pi\varepsilon_0 \frac{\Delta h}{\varepsilon_r(1-\sin\theta_0)} > \delta C. \qquad (14)$$

Using this expression, we can draw a simple sensitive plot in the relative dielectric constant–step height plane ($\varepsilon_r - \Delta h$), as shown in Fig. 11 (note that this plot is independent of apex radius and base film thickness). According to this plot, for a given capacitance noise, there exists a minimum step height $\Delta h_{\rm min}$ below which the dielectric constants cannot be experimentally detected (for instance, $\Delta h_{\rm min}=8$ nm for $\delta C=1$ aF). Similarly, for a given relative dielectric constant, there also exists a minimum step height required to make its effects appreciable. For instance, for $\varepsilon_r=3$ we have $\Delta h_{\rm min}=27$ nm for $\delta C=1$ aF and $\Delta h_{\rm min}=3$ nm for $\delta C=0.1$ aF. For the experiments reported in Fig. 9 with $\varepsilon_r=4$ and $\delta C=1$ aF, one has $\Delta h_{\rm min}>30$ nm that is larger than the thickness variation at the step of the SiO_2 structure, $\Delta h \sim 9$ nm, thus explaining why the capacitance profile is not sensitive to the value of ε_r in this measurement. Note that these conclusions are independent of the value of the apex radius and of the film thickness. Therefore, as a general rule, capacitance profile experiments on nanostructured and homogeneous thin films can be used to quantify film thickness and thickness variations at the nanoscale. However, in order to apply this approach for relative dielectric constant measurements, either higher resolution instrumentation down to subattfarad values or large roughness ($\Delta h > 30$ nm) is required.

The low sensitivity of the capacitance profiles to the relative dielectric constant can seem an inconvenient, but it turns out to be a clear advantage when the main interest is the extraction of the film thickness. This parameter can be extracted with reasonable precision without knowing the film relative dielectric constant (see an experimental example on a supported biolayer in Ref. 10).

IV. CONCLUSIONS

In the present paper we have presented a theoretical analysis of NCM on thin dielectric films. Finite-element numerical simulations have demonstrated excellent agreement with a simple logarithmic analytical model in the whole range of parameters analyzed, including tip-film separation from contact to 100 nm, film thickness from 1 nm up to 100 nm, relative dielectric constant from 1 to 100, apex radius from 30 to 200 nm, and cone angles from 10° to 45°. Based on this analytical model, we have discussed the capabilities of NCM for quantitative extraction of the local relative dielectric constant and thickness. Capacitance-distance experiments on homogeneous dielectric films can quantitatively access the local relative dielectric constant with a reasonable trade-off between tip radius and sample thickness. Capacitance profile measurements on nanostructured homogeneous thin films are suitable for quantifying the local thickness, while are less sensitive to the relative dielectric constant value. The possibility to apply this innovative and quantitative dielectric metrology in a large variety of fields, from microelectronics, material science, to biology, demands for the improvement of capacitance resolution of state-of-the-art microscopes, which is currently the main limitation.

ACKNOWLEDGMENTS

The authors would like to thank I. Casuso from University of Barcelona and Professor J. J. Saenz and E. Sahagun from Autonomus University of Madrid for fruitful discussions. This work was supported by Grant No. MAT2007-66629-C02-02 grant of the Spanish MEC.

[1] D. T. Lee, J. P. Pelz, and B. Bhushan, Rev. Sci. Instrum. **73**, 3525 (2002).
[2] L. Fumagalli, G. Ferrari, M. Sampietro, I. Casuso, E. Martinez, J. Samitier, and G. Gomila, Nanotechnology **17**, 4581 (2006).
[3] We refer as NCM to the SPM technique that probes the tip-sample capacitance in a very direct and quantitative manner by phase sensitively measuring the ac current flowing through the tip. NCM inherited its name from nanoscale impedance microscopy (Ref. 4), which employs the same current detection method to measure the tip-sample impedance. We use this name to stress the difference from the conventional SCM (Ref. 11), which normally relies on the resonant frequency method to detect variations of the tip-sample capacitance with respect to the voltage bias (dC/dV).
[4] R. Shao, S. V. Kalinin, and D. A. Bonnell, Appl. Phys. Lett. **82**, 1869 (2003).
[5] D. T. Lee, J. P. Pelz, and B. Bhushan, Nanotechnology **17**, 1484 (2006).
[6] L. Fumagalli, G. Ferrari, M. Sampietro, and G. Gomila, Appl. Phys. Lett. **91**, 243110 (2007).
[7] H. G. Tompkins and W. A. McGahan, *Spectroscopic Ellipsometry and Reflectometry: A User's Guide* (Wiley, New York, 1998).
[8] J. Graham, M. Kryzeminski, and Z. Popovic, Rev. Sci. Instrum. **71**, 2219 (2000).
[9] A. Guadarrama-Santana and A. García-Valenzuela, IEEE Trans. Instrum. Meas. **56**, 107 (2007).
[10] I. Casuso, L. Fumagalli, G. Gomila, and E. Padrós, Appl. Phys. Lett. **91**, 063111 (2007).
[11] C. C. Williams, W. P. Hough, and S. A. Rishton, Appl. Phys. Lett. **55**, 203 (1989).
[12] K. Goto and K. Hane, J. Appl. Phys. **84**, 4043 (1998).
[13] G. M. Sacha, E. Sahagun, and J. J. Sáenz, J. Appl. Phys. **101**, 024310 (2007).
[14] S. Lányi, J. Török, and P. Rehurek, J. Vac. Sci. Technol. B **14**, 892 (1996).
[15] G. M. Sacha and J. J. Sáenz, Appl. Phys. Lett. **85**, 2610 (2004).
[16] S. Hudlet, M. Saint Jean, C. Guthmann, and J. Berger, Eur. Phys. J. B **2**, 5 (1998).
[17] B. M. Law and F. Rieutord, Phys. Rev. B **66**, 035402 (2002).